SO_2 Physisorption on Exfoliated Graphite

J. L. Llanos, A. E. Fertitta, E. S. Flores, and E. J. Bottani*

Instituto de Investigaciones Fisicoquímicas Teóricas y Aplicadas (INIFTA), Casilla de Correo 16, Sucursal 4, (1900) La Plata, Argentina

Received: November 6, 2002; In Final Form: April 29, 2003

Physical adsorption of SO_2 on exfoliated graphite is studied using classical adsorption volumetry and Monte Carlo computer simulations. The experimental isotherms have been obtained in a wide temperature range to determine the critical temperature for the completion of several layers. The computer simulations are in good agreement with the experimental data. The adsorption potential is analyzed and the results are employed to interpret the distributions of adsorbed molecules according to the gas−solid energy. The adsorbed phase exhibits a certain degree of order in an incommensurate phase with respect to the graphite surface. From the simulations, the structure of the adsorbed phase is analyzed, and the unit cell edge length is estimated.

Introduction

Sulfur dioxide is an atmospheric pollutant that contributes to acid rain and other environmental problems such as corrosion and ground-level ozone formation and is linked to several respiratory diseases. SO_2 reaches the atmosphere by natural events and increasing antropogenic activity. One method of removing SO_2 from gaseous effluents is adsorption on different solids, mostly activated carbons. There are many studies concerning the adsorption of this gas on activated carbons. For example, Raymundo-Piñero et al.[1] studied the influence of an oxidation step in SO_2 adsorption, in the presence of oxygen, on activated carbons with different surface chemical composition. Guo and Chong Lua[2,3] studied activated carbons obtained from palm shells activated by KOH impregnation and by thermal activation with CO_2. Mangun et al.[4] investigated the adsorption on carbon fibers treated with ammonia. Davini[5,6] has studied SO_2 adsorption on activated carbons obtained from pitch containing iron and others obtained from bituminous coal activated by pyrolysis and CO_2 activation. Bagreev et al.[7] reported the effect of nitrogen functionality and pore size distribution on the adsorption of SO_2 on activated carbons of different origins. In all cases, the effects of pore structure and surface chemical composition have been analyzed. SO_2 chemisorption was recently studied on different solids such as NO_x adsorbents,[8] a Ag (110) face,[9] a Cu (111) face,[10] and a CsF single-crystal (100) face.[11] The electrochemical behavior of aqueous solutions of SO_2 has been recently reported by Quijada et al.[12,13] Wang and Kaneko[14,15] studied the adsorption of SO_2 on microporous carbons assuming that the pores were slit-shaped. They combined adsorption calorimetry and potential calculations to analyze the interactions of SO_2 showing the importance of dipole−dipole interactions between adsorbed molecules and the effect of specific interactions between the adsorbate and surface functional groups.

The main goal of this work is to study the adsorption of SO_2 on the flat surface of graphite combining experimental adsorption isotherms with Monte Carlo computer simulations. The employed solid is exfoliated graphite that shows a very homogeneous surface. Both the experimental and simulated adsorption isotherms are stepwise isotherms. Thus, the adsorption is studied over a wide temperature range to determine, among other properties, the critical temperatures corresponding to the formation of each layer up to the third. Computer simulations were performed at the same temperatures of the experiments, and several more have been added to compare the critical temperatures obtained to test the model employed to simulate the SO_2 molecule. The adsorption potential is analyzed, and the inferred information is employed to explain other characteristics of the adsorption.

The simulations agree quite well with the experimental isotherms, but several discrepancies are discussed. The heats of adsorption calculated from the experiments are in agreement with the ones calculated from the simulations. The cross-sectional area of the adsorbate estimated from both the experiment and simulation agree with values recommended in the literature or calculated from models.[16] Other properties characterizing the behavior of the adsorbed film are also discussed. The partially ordered structure of the adsorbed phase is analyzed.

Experimental Details

The adsorption isotherms have been determined using conventional volumetric equipment. Pressure transducers were employed to determine the pressure, and digital thermometers were used to measure both the ambient and bath temperatures. The employed exfoliated graphite sample has a N_2 BET surface area of 45 m^2/g, and it has been employed uncompressed. Before the adsorption of SO_2, the sample was degassed at 600−650 K for 10 h under high vacuum. The obtained isotherms are fully reversible over the entire pressure range studied for each isotherm. This fact rules out the possible chemisorption of SO_2. One interesting characteristic of the adsorption process is the time required to achieve equilibrium, which is very long even at low pressures. The cryogenic baths were obtained using several substances at their melting points. SO_2 vapor pressure has been calculated with eq 1,[17] and the obtained values are consistent with the simulations and experimental results.

$$\log_{10} P[\text{Torr}] = 8.3423 - \frac{1434.9}{T[\text{K}]} \qquad (1)$$

* Corresponding author. E-mail: ebottani@inifta.unlp.edu.ar. Fax: 54-221-425-4642. Phone: 54-221-425-7430.

10.1021/jp0273981 CCC: $25.00
Published on Web 07/09/2003

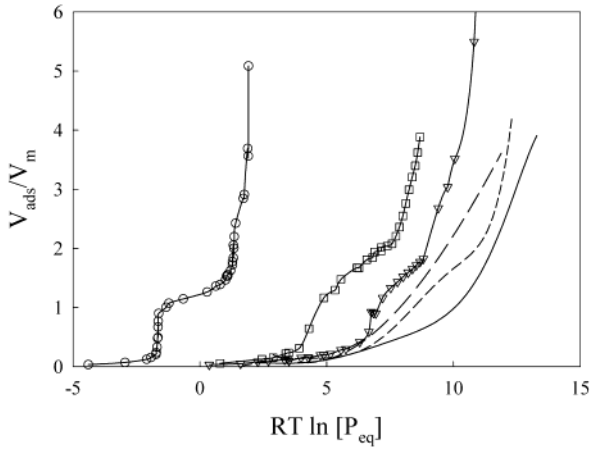

Figure 1. SO_2 experimental adsorption isotherms on exfoliated graphite. The temperature corresponding to each isotherm goes from left to right: 189.2, 229, 243.2, 251.7, 259.7, and 273.2 K. V_m is the BET monolayer capacity, and P is in Torr.

TABLE 1: Interaction Parameters Employed to Calculate Gas−Solid and Gas−Gas Interactions

sites	ϵ [K]	σ [nm]
S−S	252.0	0.429
O−O	74.8	0.3027
S−O	137.3	3.66
S−C(graphite)	87.5	0.405
O−C(graphite)	45.8	0.316

The experimental vapor pressure obtained from the isotherms differs by less than 1% from the values calculated with eq 1. The difference between the experimental vapor pressures and the ones obtained from the simulated isotherms is less than 1% at 77.5 K, but at higher temperatures, there is a larger difference. These differences are due to inaccuracy in eq 1 and the fact that the simulations are not very reliable at pressures close to saturation. The set of experimental adsorption isotherms are shown in Figure 1, where for the sake of clarity not all of the experimental points have been included and have been replaced by lines drawn through them.

Simulation Details

Grand canonical Monte Carlo simulations have been performed using the algorithm previously described.[18] Each configuration is the result of 2.7×10^9 attempts of the standard movements and creation/destruction steps, for which the average acceptance ratio was kept nearly constant (1−2% for creation/destruction and 40−50% for movements). The adsorbate molecule is modeled as a rigid set of three Lennard-Jones interaction sites located on the atoms. The S−O bond length is 0.143 nm, and the O−S−O angle is 119.5°. The SO_2 dipole moment is modeled by placing partial charges on each atom. These charges have been calculated using the MP2 method, and the values produced by the employed software[19] were $q_S = 0.813622$ and $q_O = -0.406811$, which produce a dipole moment $\mu = 1.68$ D in good agreement with the experimental value ($\mu = 1.63$ D).

Lateral interactions include dispersion and electrostatic terms, and the employed gas−solid potential has been developed by Steele[20] using a corrugation factor of 1.5. The interaction parameters employed to calculate all of the interactions are quoted in Table 1. Mixed parameters have been calculated using the Lorentz−Berthelot combining rules. After trial simulation runs, the original parameters have been modified to fit the experimental isotherms. The orientation of the adsorbate is described with Euler's angles formalism as has been previously described elsewhere.[21] The gas−solid potential for an isolated molecule exhibits three minima depending on the orientation of the molecule relative to the surface. The minima occur at approximately the same distance from the surface, ca. 0.39 nm. The energy values are 23.5 kJ/mol for the molecule with its molecular plane perpendicular to the surface and the oxygen atoms pointing away from the surface. The second minima, 31.2 kJ/mol, corresponds to the molecule in the same orientation but with the oxygen atoms pointing toward the surface, and the third minima, 26.8 kJ/mol, corresponds to the molecule lying flat on the surface. These values give an average energy of 27.2 kJ/mol, which is in agreement with other results, as will be discussed later.

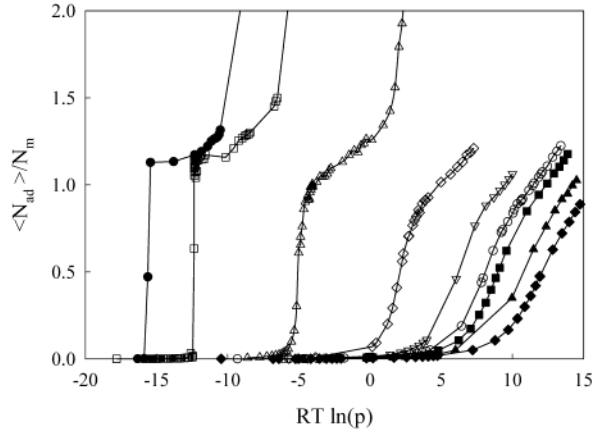

Figure 2. SO_2 simulated isotherms on the basal plane of graphite. The temperature corresponding to each isotherm goes from left to right: 77.5, 100, 150, 200, 229.2, 243.2, 250, 263.2, and 273.2 K. N_m is the BET monolayer capacity, and P is in Torr.

A rectangular simulation box with an area of 23.46 nm^2 has been employed for all of the simulations. Periodic boundary conditions have been applied in both x and y directions and a rigid plane conveniently located closed the simulation box in the z direction.

Results and Discussion

Even though the experimental isotherms show the formation of several adsorbed layers, we will focus our discussion on the first layer. Portions of the simulated adsorption isotherms are shown in Figure 2. The agreement between the simulations and experiments is good.

The cross-sectional area of SO_2 is a rather complicated problem. In fact, using the experimental isotherms, we found that the specific surface area calculated with the BET method gives the same value as the one obtained with N_2 (45 m^2/g) if a cross-sectional area equal to 0.242 nm^2 is employed for SO_2. This cross-sectional area is an average over all of the temperatures studied. The maximum obtained value is 0.319 nm^2 (at 189.2 K), the minimum, 0.196 nm^2 (at 243.2 K), and an intermediate value, 0.212 nm^2 (at 229.2 K). These values are of the same order of magnitude as other reported results[16] that are as low as 0.13 nm^2 and up to 0.271 nm^2. From simple molecular models, another set of values are obtained. For the molecule lying flat on the surface, the cross-sectional area is $\sigma_{flat} = 0.246$ nm^2; for the molecule with the oxygen atoms on the surface and the sulfur atom above them, the cross-sectional area is $\sigma_{per} = 0.169$ nm^2. If the molecule is vertical with an oxygen atom close to the surface and assuming cylindrical symmetry, the cross-sectional area is minimal and equal to $\sigma_{ver} = 0.11$ nm^2. From the analysis of the configurations generated

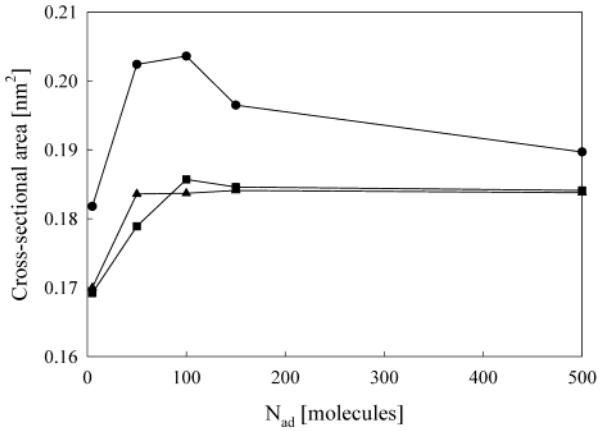

Figure 3. SO_2 cross-sectional area at 50 (○), 100 (□), and 229.2 K (△).

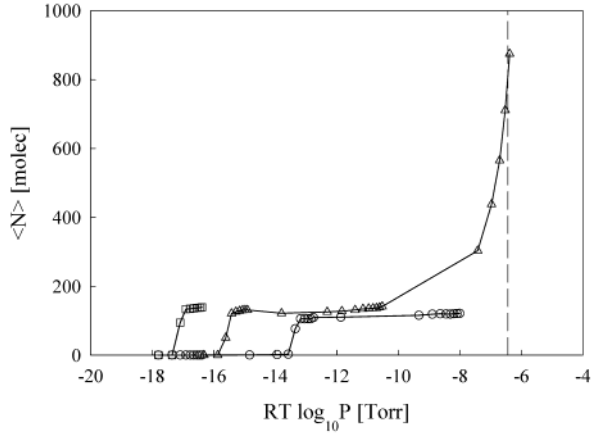

Figure 4. Simulated isotherms using different dipole moment values. (□) Dipole-altered $q_S = 1$ and $q_O = -0.50$, (○) = 0, and (△) $\mu = 1.68$ D as employed in the other simulations. The vertical broken line indicates the vapor pressure calculated with eq 1.

during the simulations, it is possible to calculate the average cross-sectional area at each temperature as a function of the number of adsorbed molecules. The profiles obtained at three temperatures are shown in Figure 3, and the monolayer capacity is ca. 100 molecules. The value obtained at 50 K near the monolayer completion is almost equal to the average cross-sectional area between σ_{per} and σ_{flat}, whereas at 100 and 229.2 K the cross-sectional area is close to the average of the three orientations described. At very low surface coverage, the value obtained at 100 and 229.2 K is equal to σ_{per}, and at 50 K, it is close to the average between σ_{per} and σ_{ver}. These results are in agreement with the snapshots that are presented later on.

From the microdensity profiles that will be discussed later, the thickness of a monolayer can be estimated. The obtained value, 0.52 ± 0.07 nm, is in excellent agreement with the average diameter estimated from viscosity measurements (0.54 nm)[22] and the valued deduced from the van der Waals constants (0.56 nm).

Another test performed to determine the accuracy of our SO_2 model consisted of simulating the adsorption using different values for the dipole moment. One simulation was run by neglecting the dipole moment, and another one was run with the charges located on each atom altered ($q_S = 1.$ and $q_O = -0.50$). The obtained isotherms at 77.5 K are shown in Figure 4. As can be seen in the Figure, the dipole moment exerts a large influence on the position of the adsorption isotherm, mainly by determining the vapor pressure of the model

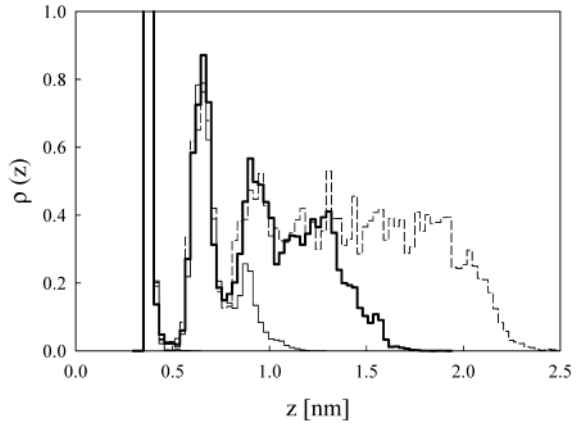

Figure 5. Density profiles obtained at 77.5 K. The number of adsorbed molecules is $\langle N \rangle = 125.66$; this line is masked by the others because it is located under the first peak; $\langle N \rangle = 303.41$ (thin line), $\langle N \rangle = 565.05$ (thick line), and $\langle N \rangle = 874.81$ (broken line).

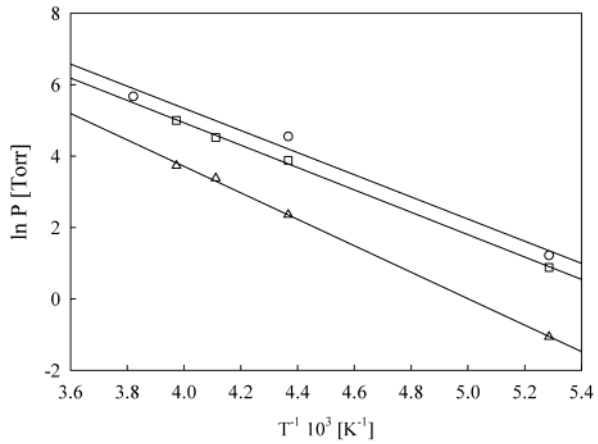

Figure 6. Experimental values of the transition pressures as a function of the inverse temperature for the formation of the first three layers. (△) First layer, (□) second layer, (○) third layer.

adsorbate. Another detected difference concerns the attained monolayer capacity, which increases as the dipole moment increases. In the example shown in Figure 4, the first step in the isotherms indicates a monolayer capacity ranging from ca. 100 molecules for $\mu = 0$ up to 150 molecules for the increased dipole moment isotherm. This result is expected because changes in the dipole moment must alter the interactions between the adsorbed molecules. As the dipole moment is increased, the molecules could be more densely packed, resulting in a large monolayer capacity and in an augmented gas−gas interaction energy. An interesting feature is that the step character of the isotherm seems to be independent of the dipole moment value.

The microdensity profiles obtained at 77.5 K are shown in Figure 5. It is possible to identify up to three layers, in agreement with what is seen in the corresponding adsorption isotherm. Only the first layer is clearly separated from the others. (Note the deep minima between the first and second peak.) The separation of the second and third layers is not sharp, indicating some degree of disorder in the adsorbed phase even at this low temperature. The microdensity profiles obtained with the other dipole moment values show the same behavior with respect to the separation of the second and upper layers.

Both sets of adsorption isotherms, experimental and simulated, have been employed to calculate the adsorption enthalpies and critical temperatures for the formation of each layer up to the third. The analysis has been performed following the classical treatment reported by Menaucourt et al.[23] Figure 6

depicts the experimental values of the transition pressures as a function of the inverse temperature for the first three layers. From the slope of each line, the adsorption enthalpy is obtained. The obtained values for the first, second, and third layers are −30.8, −26.0, and −25.8 kJ/mol, respectively. The value obtained for the first layer is in perfect agreement with the minimum in the adsorption potential for the adsorbed molecule lying flat on the surface. The value obtained for the third layer is close to the vaporization enthalpy of pure SO_2 at the boiling point (24.9 kJ/mol) and is in good agreement with the experimental value reported by Wang and Kaneko[14] for SO_2 adsorption on nonporous carbon black. The intercept of the lines is the entropy of adsorption. The average value for the three layers is 0.14 kJ mol^{-1} K^{-1}, which is almost identical to the theoretical value (0.145 kJ mol^{-1} K^{-1}) calculated for the adsorbate with two translational degrees of freedom plus three rotational degrees of freedom and one vibrational degree of freedom.[14]

The same analysis performed with the simulated isotherms gives the following results. The average adsorption enthalpy is 26.8 kJ/mol, which is in excellent agreement with the average value obtained from the experimental isotherms (27.5 kJ mol^{-1}). The entropy of adsorption is 0.14 kJ mol^{-1} K^{-1}, which is the same value obtained from the experiments. These results confirm not only the validity of the simulations but the main characteristics of the adsorbed layer.

The set of adsorption isotherms can be employed to determine the critical temperatures corresponding to the condensation in the first and upper layers. In fact, the critical temperature is the maximum temperature for which the steps of the isotherms are still vertical (i.e., the slope of the isotherm (dp/dT) is zero if the transition is first order[24]). The calculation of the derivatives is not very accurate and presents several practical problems. Nevertheless, the method applied to the experimental isotherms gives $T_C^{2D} = 242$ K for the first layer, and $T_C^{2D} = 228$ K for the second layer. The simulated isotherms give a critical temperature for the first layer of $T_C^{2D} = 240$ K. Unfortunately, the statistical errors in the simulations combined with the experimental errors and the inaccuracy of the derivatives do not allow us to calculate a reliable critical temperature for the other layers. The obtained critical temperatures are consistent with what is observed on the adsorption isotherms. The ratio between the 2D and 3D critical temperatures has the same value for both the simulations and experiments and is equal to 0.56, which is close to the value obtained from mean-field theory (0.5).[25,26]

Another interesting property that can be derived from the isotherms is the critical exponent, whch has different values according to the dimensionality of the system.[24] The critical exponents control the behavior of several thermodynamic magnitudes in the neighborhood of the critical temperature. For example, the exponent β appearing in the relationship giving the change in the adsorbed amount during the transition, $N^h - N^L$, as a function of $T - T_C$ is

$$\ln(N^h - N^L) = \ln(DN_m) + \beta \ln\left(\frac{T_C - T}{T_C}\right) \qquad (2)$$

where N^L and N^h are the adsorbed amounts at the beginning of the step and at the top of the step, respectively, D is a constant, and N_m is the monolayer capacity. The results obtained for the simulated isotherms are shown in Figure 7. The critical exponent obtained from the slope of the regression line is $\beta = 0.35$ with a correlation coefficient of $r^2 = 0.99$. Given the uncertainties

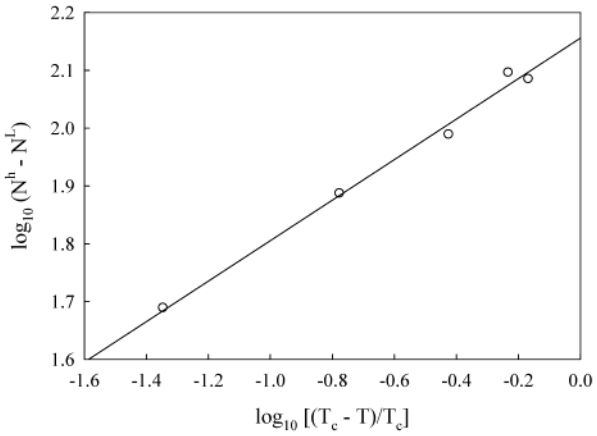

Figure 7. Critical exponent obtained from the simulated adsorption isotherms.

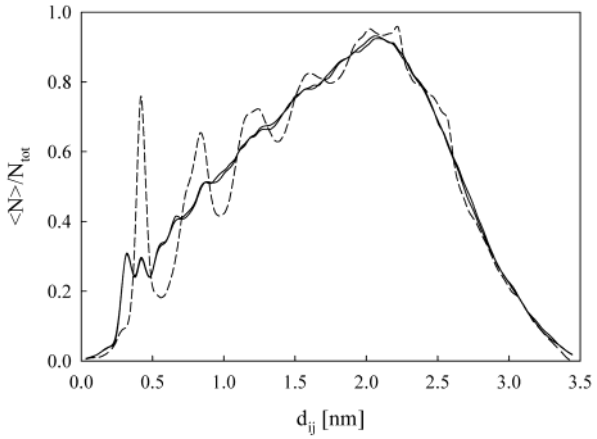

Figure 8. Profiles depicting the average number of adsorbed molecules as a function of the distance corresponding to an ordered structure. The broken line corresponds to the S_i-S_j distance, and the full lines that are almost identical correspond to $O1_i-O1_j$ and $O2_i-O2_j$ distances. The number of adsorbed molecules was in all cases 150.

in the determination of the critical exponent,[27] we will not comment further on this point except to note that the obtained value is close to the one expected for the 3D Ising model ($\beta = 0.33$).

We will now discuss the structure of the adsorbed layer considering only the molecules that technically belong to the first layer. A molecule is considered to be in the first layer when the sulfur atom is located below 0.45 nm, disregarding the position of the oxygen atoms. This criterion is consistent with the thickness of the adsorbed layer and the distance at which the gas−solid potential is a minimum.

The configurations generated during the simulations have been analyzed by calculating the distance between sulfur atoms of different molecules, on one side, and between the oxygen atoms. Then, the distances were referred to the graphite unit cell dimensions, and histograms were constructed in the following way. For each molecule, the position were a neighbor should be located in a perfectly ordered structure was calculated. Then, this position was compared with the actual location of the other molecules in the configuration, and each time a molecule was found to be in the right location, with a tolerance of 0.01 nm, it was counted in the histogram. The resulting number of molecules was averaged over all configurations and finally divided by the total number of adsorbed molecules. This was done for the sulfur atoms and both oxygen atoms of the molecule. The results indicate that the adsorbed molecules in

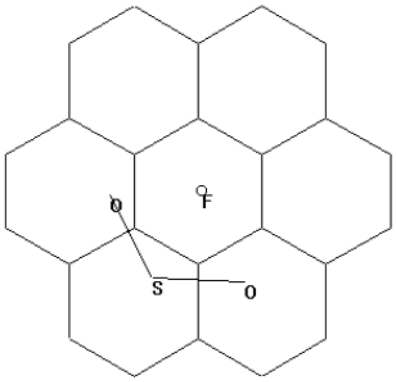

Figure 9. Schematic representation of an adsorbed molecule, flat on the surface. The picture is to scale, and the distance between the S atom and the origin of the unit cell of the solid surface, indicated by point F, is 0.189 nm.

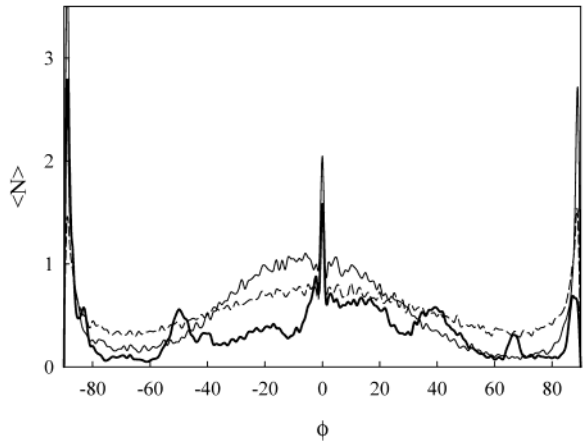

Figure 10. Distributions of molecules according to the in-plane rotational angle, ϕ, near the monolayer and for temperatures 50 K (thick line), 100 K (thinner line), and 229 K (broken line).

TABLE 2: Location of the S−S and O−O Atoms' Distance Peaks Obtained by Averaging the Equilibrated Configurations[a]

T [K]	S_i-S_j [nm]	$O1_i-O1_j$ [nm]	$O2_i-O2_j$ [nm]
50	0.42	0.32	0.42
		0.55−0.57	
		0.67	
	0.84	0.87	0.87
	1.26	1.22−1.24	
	1.57	1.57	
100	0.42	0.32	0.42
		0.64	0.64
	0.84	0.87	0.87
	1.26	1.28	1.28
	1.68		
229.2	0.42	0.42	0.42
	0.84		
	1.26		

[a] S_i-S_j is the distance between sulfur atoms, and $O1_i-O1_j$ and $O2_i-O2_j$ are the distances between the oxygen atoms.

the first layer form an ordered structure determined by the sulfur atoms. Figure 8 shows as an example the profile obtained at 100 K. The profiles obtained at other temperatures are very similar, and the locations of the different peaks obtained at three temperatures are quoted in Table 2. The curves corresponding to the oxygen atoms are almost coincident in all of the studied cases. From these results, it is possible to estimate the edge length of the SO_2 unit cell, and the result is 0.297 nm. The

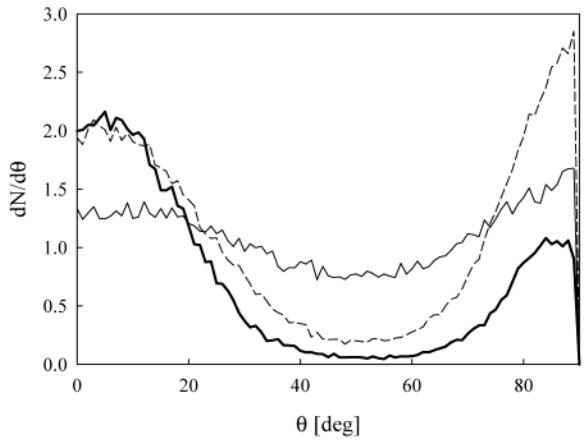

Figure 11. Distributions of molecules according to the tilt angle, θ, at a surface coverage close to the monolayer and temperatures 50 K (thick line), 100 K (broken line), and 229 K (thinner line).

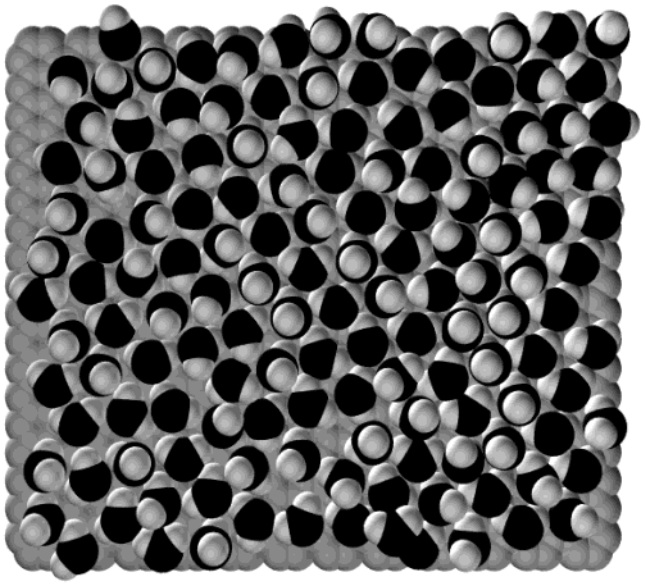

Figure 12. Snapshot of the adsorbed phase at 77.5 K. Black spheres represent sulfur atoms, bright-gray spheres represent oxygen atoms, and light-gray spheres represent the first layer of the graphite surface. The adsorbed amount is close to the monolayer completion.

edge of this unit cell is ca. 20% larger than the graphite unit cell (0.246 nm). According to our results, the sulfur atoms are arranged in this incommensurate phase at all temperatures analyzed up to 229.2 K. Moreover, the order persists at long distances up to 100 K. With respect to the position of the oxygen atoms, a certain order is also inferred from the obtained histograms. Nevertheless, it can be considered to be short-range order. It must be pointed out that the conclusions concerning the order in the structure of the oxygen atoms is very approximate because we have not discriminated the atoms according to their *z* coordinates. Thermal agitation seems to prevent the adoption of an ordered in-plane structure with respect to the oxygen atoms even at 50 K. (See the snapshots discussed later.)

The calculated average in-plane distance between a sulfur atom and the center of a graphite hexagon is almost constant. The obtained value is $\langle d \rangle = 0.187 \pm 0.001$ nm, and it is independent of the temperature. Figure 9 shows a schematic representation of the configuration of an SO_2 molecule on the graphite surface. The orientation of the molecule was selected on the basis of the average distance calculated for the oxygen

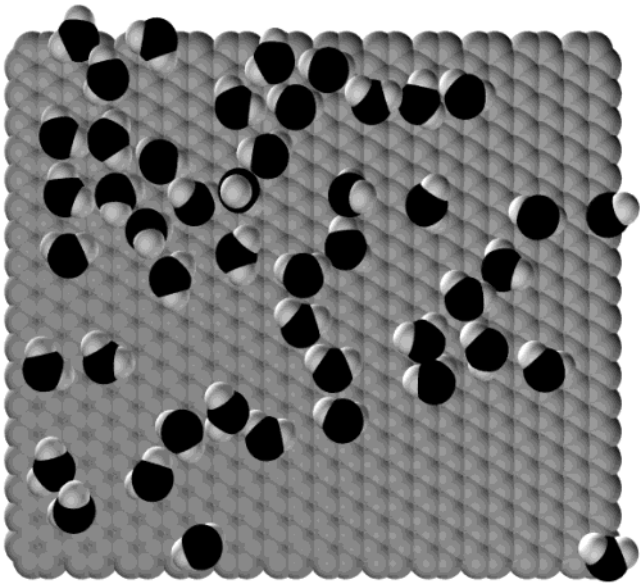

Figure 13. Same as Figure 12 but with 46 adsorbed molecules.

atoms with respect to the center of the hexagon. Moreover, this configuration agrees with results obtained for the distribution of molecules over the rotation angle ϕ. Figure 10 depicts the distributions obtained at three temperatures and surface coverage close to the monolayer. It can be seen that there are three main peaks corresponding to 0 and $\pm 90°$ with respect to the coordinate system. At 50 K, other peaks are observed because of the smaller kinetic energy content of the adsorbate molecules. Figure 11 shows the distributions of molecules with respect to the tilt angle, θ, obtained at the same coverage and temperatures of Figure 9. The distributions have two main peaks located close to 0° (the molecule lies flat on the surface) and 90° (the sulfur atom is above the oxygen atoms). These results are confirmed by the snapshots obtained during the simulations. Figure 12 shows one snapshot corresponding to a surface coverage close to the monolayer, and Figure 13 shows one obtained with fewer adsorbed molecules. The snapshot shown in Figure 12, obtained at 77.5 K, shows the molecules in the structure previously described. It is also observed that there is no orientational order. Even at surface coverages much lower than a monolayer, the adsorbed molecules are not completely flat on the surface, as can be seen in Figure 13.

Conclusions

The cross-sectional area of SO_2 adsorbed on the basal plane of graphite presents a maximum value of 0.319 nm^2 (at 189.2 K), and the minimum value, 0.196 nm^2, was obtained at 243.2 K. These values are in agreement with the one obtained from the experimental isotherms and using the BET model. The thickness of the monolayer has been estimated to be 0.52 ± 0.07 nm, in excellent agreement with values obtained from different sources (viscosity measurements and van der Waals constants). The simulations performed using different values for the dipole moment of the adsorbate show that it has two main effects on the adsorption isotherms. It strongly affects the vapor pressure and, to a lesser extent, the monolayer capacity. An interesting fact is that the step character of the isotherm is preserved. The experimental and simulated isotherms have been employed to determine the heat of adsorption and the critical temperatures for the completion of several layers. The agreement between the experiments and simulations is quite good and confirms the model employed to simulate the system. The critical exponent for the transition corresponding to the first layer indicates that the system exhibits universality. Because of the large uncertainty involved in the determination of the critical exponent, we do not discuss this fact in more detail. The adsorbed phase exhibits an ordered structure determined by the sulfur atoms. Thermal kinetic energy, even at 50 K, prevents the formation of a more ordered structure involving the position of the oxygen atoms. Even though our simulations reproduce quite well several magnitudes of the systems, the structure of the adsorbed phase should be confirmed using other techniques, as has been done with other systems. More extensive computer simulations are under development to study the 2D critical behavior of SO_2 adsorbed on the basal plane of graphite.

Acknowledgment. E.J.B. is Professor of the Universidad Nacional del Litoral. Financial support is granted by Consejo Nacional de Investigaciones Científicas y Técnicas (CONICET), Comisión de Investigaciones Científicas de la Provincia de Buenos Aires (CIC), and Universidad Nacional de La Plata (UNLP).

References and Notes

(1) Raymundo-Piñero, E.; Cazorla-Amorós, D.; Salinas-Martínez de Lecea, C.; Linares-Solano, A. *Carbon* **2000**, *38*, 335.
(2) Guo, J.; Chong Lua, A. *J. Chem. Technol. Biotechnol.* **2000**, *75*, 971.
(3) Guo, J.; Chong Lua, A. *J. Colloid Interface Sci.* **2002**, *251*, 242.
(4) Mangun, C. L.; DeBar, J. A.; Economy, J. *Carbon* **2001**, *39*, 1698.
(5) Davini, P. *Carbon* **2001**, *39*, 2173.
(6) Davini, P. *Carbon* **2001**, *39*, 1387.
(7) Bagreev, A.; Bashkova, S.; Bandosz, T. J. *Langmuir* **2002**, *18*, 1257.
(8) Mahzoul, H.; Limousy, L.; Brilhac, J. F.; Gilot, P. *J. Anal. Appl. Pyrolysis* **2000**, *56*, 179.
(9) Zhu, P.; Tang, J. C.; He, J. P. *Phys. Chem. Chem. Phys.* **2000**, *2*, 1123.
(10) Jackson, G. J.; Driver, S. M.; Woodruff, D. P.; Abrams, N.; Jones, R. G.; Butterfield, M. T.; Crapper, M. D.; Cowie, B. C. C.; Formoso, V. *Surf. Sci.* **2000**, *459*, 231.
(11) Heidberg, J.; Henseler, H. *Surf. Sci.* **1999**, *427*, 439.
(12) Quijada, C.; Morallón, E.; Vázquez, J. L.; Berlouis, L. E. A. *Electrochim. Acta* **2000**, *46*, 651.
(13) Quijada, C.; Huerta, F. J.; Morallón, E.; Vázquez, J. L.; Berlouis, L. E. A. *Electrochim. Acta* **2000**, *45*, 1847.
(14) Wang, Z. M.; Kaneko, K. *J. Phys. Chem.* **1995**, *99*, 16714.
(15) Wang, Z. M.; Kaneko, K. *J. Phys. Chem. B* **1998**, *102*, 2863.
(16) Mikhail, R. Sh.; Robens, E. In *Microstructure and Thermal Analysis of Solid Surfaces*; Wiley & Sons: 1983; Appendix C, p 433.
(17) L'Air Liquide. *Encyclopèdie des Gaz.* Elsevier: New York, 1976; p 1121.
(18) Tascón, J. M. D.; Bottani, E. J. *J. Phys. Chem. B* **2002**, *106*, 9522.
(19) Frisch, M. J.; Trucks, G. W.; Schlegel, H. B.; Gill, P. M. W.; Johnson, B. G.; Robb, M. A.; Cheeseman, J. R.; Keith, T.; Petersson, G. A.; Montgomery, J. A.; Raghavachari, K.; Al-Laham, M. A.; Zakrzewski, V. G.; Ortiz, J. V.; Foresman, J. B.; Cioslowski, J.; Stefanov, B. B.; Nanayakkara, A.; Challacombe, M.; Peng, C. Y.; Ayala, P. Y.; Chen, W.; Wong, M. W.; Andres, J. L.; Replogle, E. S.; Gomperts, R.; Martin, R. L.; Fox, D. J.; Binkley, J. S.; Defrees, D. J.; Baker, J.; Stewart, J. P.; Head-Gordon, M.; Gonzalez, C.; Pople, J. A. *Gaussian 94*, revision D.1; Gaussian, Inc.: Pittsburgh, PA, 1995.
(20) Steele, W. A. *Surf. Sci.* **1973**, *36*, 317.
(21) Bertoncini, C.; Odetti, H.; Bottani, E. J. *Langmuir* **2000**, *16*, 7457.
(22) Kaneko, K. In *Adsorption on New and Modified Inorganic Sorbents.* Dąbrowski, A., Tertykh, V. A., Eds.; Studies in Surface Science and Catalysis; Elsevier, Amsterdam, 1996; Vol. 99, p 573.
(23) Menaucourt, J.; Thomy, A.; Duval, X. *J. Chim. Phys.* **1980**, *77*, 959.
(24) Larher, Y. *Mol. Phys.* **1979**, *38*, 789.
(25) Bienfait, M. In *Phase Transitions in Surface Films*; Dash, J. G., Ruvalds, J., Eds.; NATO Advanced Study Institutes Series B: Physics; Plenum Press: New York, 1980; Vol. 51, p 29.
(26) Persson, B. N. J. *Surf. Sci. Rep.* **1992**, *15*, 1.
(27) Nicholson, D.; Parsonage, N. G. In *Computer Simulation and the Statistical Mechanics of Adsorption*; Academic Press: New York, 1982; Chapter 2.